

DESIGN OF A SOFTWARE TO ASSESS THE IMPACT OF A SPACE MISSION ON THE SPACE ENVIRONMENT

Camilla Colombo⁽¹⁾, Mirko Trisolini⁽¹⁾, Juan Luis Gonzalo⁽¹⁾, Lorenzo Giudici⁽¹⁾, Stefan Frey⁽²⁾, Emma Kerr⁽³⁾, Noelia Sánchez-Ortiz⁽³⁾, Francesca Letizia⁽⁴⁾, Stijn Lemmens⁽⁴⁾

⁽¹⁾ *Dep. of Aerospace Science and Technology, Politecnico di Milano, Via la Masa 34, 20156 Milano, Italy, Emails: camilla.colombo@polimi.it, mirko.trisolini@polimi.it, juanluis.gonzalo@polimi.it, lorenzo1.giudici@polimi.it*

⁽²⁾ *Vyoma, Eckhardtstraße 28, 64289 Darmstadt, Germany, Email: stefan.frey@vyoma.space*

⁽³⁾ *Deimos Space, Harwell Innovation Centre, Fermi Avenue, Harwell Oxford, OX11, OQR Oxfordshire, UK, Emails: emma.kerr@deimos-space.com, noelia.sanchez.ortiz@gmail.com*

⁽⁴⁾ *European Space Agency, Space Debris Office, Robert-Bosch-Str. 5, 64293 Darmstadt, Germany, emails: Francesca.Letizia@esa.int, Stijn.Lemmens@esa.int*

ABSTRACT

In this paper we will present the design of a software to assess the impact of a space mission on the space environment and its contribution to the space overall capacity developed within an ESA-funded study by Politecnico di Milano and Deimos Space. The aim of this project is to create an open software platform for the evaluation of the impact of space missions on the space environment for a future sustainability of the access to space. The impact on the environment of a space object is assessed based on mission information such as its orbit, mass, cross-section, and on the risk of fragmentation due to accidental collisions or break-up.

1 INTRODUCTION

Space, as any other ecosystem, has a finite capacity. The continuous growth of space activities, due to the increasing reliance of our daily lives on services from Space, the privatisation of the space market and the lower cost of deploying smaller and distributed missions in orbit, is from one side improving human-life quality and however, it is contributing to overloading this delicate ecosystem. Is interesting to note as the orbital environmental trend, represented by the space debris growth has a similar behaviour to the Earth system trends which are the environmental trends [1]. As of today, the space debris problem is internationally recognised, and thus the environmental concern in Space activities is becoming a priority. For example, the European Space Agency (ESA) successfully applied life cycle assessment of spacecraft from launch from disposal. The environmental impact of spacecraft and launcher manufacturing and operation was assessed, as well as ground segment activities to reduce the impact of “pollution” in orbit, in the atmosphere and on ground [2]. Several environmental indices have been introduced over the years to assess the status of the space environment [11,12,13]. These indices take into account distinct aspects of the space debris environment, but they focus on monitoring the possible increase in the

number of objects in space, and on the risk they pose to current and future satellites.

In this paper we will present the design of a software to assess the impact of a space mission on the space environment and its contribution to the Space overall capacity [8], developed within an ESA-funded study by Politecnico di Milano and Deimos Space. Indeed, the aim of this project is to create an open software platform for the evaluation of the impact of space missions on the space environment for a future sustainability of the access to space. The impact on the environment of a space object is assessed based on mission information such as its orbit, mass, cross-section, and on the risk of fragmentation due to accidental collisions or break-up. The contribution of the launching stages to the mission impact assessment is also considered. The output of the environmental analysis is summarised into a single score, suitable for its integration into a life cycle assessment procedure. The top-level goals for this project are:

- To analyse the state-of-the-art on cloud propagation, address its gaps and aim for its extension to any orbital regions;
- To develop a database to track, update and analyse the objects in orbit and gather the information needed for a space environment impact assessment;
- To develop a workflow for the computation of the environment capacity and implement it into a software pipeline;
- To develop a web-based interface for the submission and evaluation of the space environmental assessment based on the technology developed in this study.

The paper will present the development and consolidation of the different building blocks required for the definition of the environmental capacity. An overview of the expected user interface functionalities will also be presented.

2 CLOUD PROPAGATION APPROACH

2.1 Fragment propagation approach

The phase space density is propagated using the continuity equation:

$$\frac{\partial n}{\partial t} + \nabla(n \mathbf{F}) = 0 \quad (1)$$

where t is the time, n the phase space density, \mathbf{x} the phase space variables, and $\mathbf{F} = \frac{d\mathbf{x}}{dt}$ the dynamics.

The density is numerically propagated using the method of characteristics along with the phase, to achieve efficient integration while remaining applicable to any orbital region and force model. In this way Eq. (1) is transformed from a partial differential equation into a system of ordinary differential equations. The initial characteristics, defined by a point in the phase space and its density, are sampled from the initial distribution.

The trajectories are sampled from the initial distribution and propagated in the full orbital element set plus area-to-mass ratio, A/m [1]. Then the spatial density and impact rate is evaluated at any required time. Different methods will be investigated for the density estimation: a pure sample-based Monte Carlo (MC) method for validation purposes, a weighted Monte-Carlo method based on the propagation of the characteristic lines and binning for describing the whole domain (see Section 2.2) and a Gaussian mixture-model surrogate model proposed in [6]. For the first part of the project the first two methods have been implemented; one of the main challenges is the memory allocation for the propagation of a 6D domain when including the orbital elements and the are-to-mass ratio. This is tackled exploiting the properties of sparse matrices as will be described in Section 2.2.

2.2 Sparse matrix approach for binning

The fragment propagation approach described in Section 2.1 propagates the fragments density along the characteristics. If propagated to the same epoch, the characteristics form a scattered point cloud in the phase space domain. Therefore, a density interpolation technique, to get a picture of the density distribution in the whole domain, is required. In this work, an equally-sized binning approach is proposed. The estimation of the density through binning in a six-dimensional space is a tremendous challenge from a memory usage standpoint. However, in most of the cases, the debris generated by a fragmentation event remain bounded in certain regions of the phase space. Hence, a Compressed-Row-Storage (CRS) technique is applied to the highly-sparse bins matrices to conveniently store the

density distribution [3]. The Extended Karnaugh Map Representation (EKMR) [4] is used to transform the six-dimensional array of density values into a series of two-dimensional matrices, as shown in Figure 1.

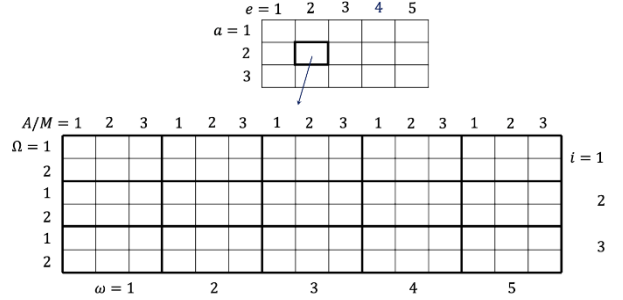


Figure 1: EKMR scheme.

It is worth noticing that in principle it would be possible to concentrate the whole phase space domain in one two-dimensional array; however, this would imply to process a matrix of dimension $\prod_{j=1}^3 N_j \times \prod_{j=4}^6 N_j$, with N_j the number of bins in the j^{th} variable, that would cause to run out of memory in most of the cases.

The CRS technique is then applied to the set of two-dimensional arrays, further re-shaping the density distribution into three vectors for each of the sub-domain of the phase space, representing:

- The non-zero density values taken in row-wise fashion.
- The column position of the non-empty bins.
- The pointers to the first non-zero element of each row and an additional element that counts the number of non-zero elements N_{nze} .

A qualitative analysis can be performed to assess the minimum sparse ratio S required to make the CRS technique convenient from a memory usage viewpoint, where the sparse ratio of a matrix is the ratio between the non-zero elements and the total number of its elements. The CRS technique is convenient whenever the total number of elements stored is lower than the number of elements in the six-dimensional array. Referring to the arbitrary EKMR scheme of Figure 1, the number of elements stored is:

$$El_{CRS} = \sum_{j=1}^{N_a N_e} (2N_{nze}^j + N_i N_\Omega + 1) \quad (2)$$

where N_a , N_e , N_i and N_Ω are the number of bins in semi-major axis, eccentricity, inclination, and right ascension of the ascending node, respectively, and N_{nze}^j is the number of non-zero elements of the j^{th} two-dimensional array. Adopting the sparse ratio S , Eq. (2) can be rearranged as:

$$El_{CRS} = \sum_{j=1}^{N_a N_e} \left(2S_j N_i N_\Omega N_\omega N_{A/M} + N_i N_\Omega + 1 \right) \quad (3)$$

$$= 2N_i N_\Omega N_\omega N_{A/M} \sum_{j=1}^{N_a N_e} S_j + N_a N_e (N_i N_\Omega + 1)$$

where N_ω and $N_{A/M}$ are the number of bins in argument of periapsis and area-to-mass ratio, respectively, and S_j is the sparse ratio of the j^{th} two-dimensional array. The following assumptions are introduced:

- The phase space domain is equally partitioned in N bins along every hyper-direction.
- An average sparse ratio \bar{S} is assumed for each two-dimensional array.

Under these hypotheses, Eq. (3) reduces to:

$$El_{CRS} = 2\bar{S}N^6 + N^2(N^2 + 1) \quad (4)$$

The expression of Eq. (4) must be compared with the total number of elements N^6 in the six-dimensional array, leading to the following requirement for the average sparse ratio \bar{S} :

$$\bar{S} < \frac{1}{2} - \frac{N^2 + 1}{2N^4} \quad (5)$$

Figure 2 shows the behaviour of \bar{S} as function of the number of bins N in each hyper-direction; as it can be noticed, the curve asymptotically approaches $\bar{S} = 0.5$ for $N > 20$, meaning that whenever more than half of the bins are empty, the CRS technique is convenient from a memory usage standpoint.

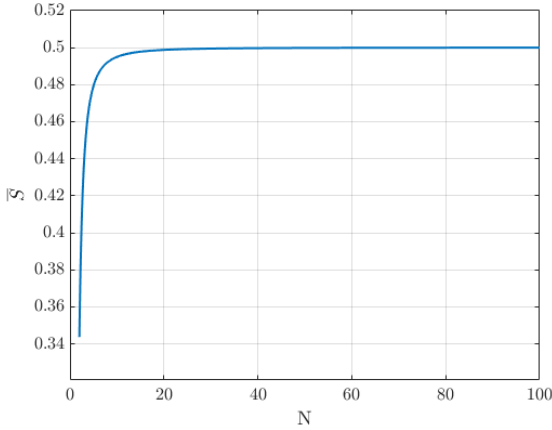


Figure 2: Average sparse ratio as function of the number of bins in each hyper-direction.

Finally, it is worth observing that the way the EKMR scheme is built affects the number of elements stored. Referring to the scheme of Figure 1, the number of bins for each phase space variable are selected as follows:

$$N_a = N_e = N_1, \quad N_i = N_\Omega = N_2, \quad N_\omega = N_{A/M} = N_3$$

The number of stored elements of Eq. (3), still considering the average sparse ratio \bar{S} , reduces to:

$$El_{CRS} = 2\bar{S}N_1^2 N_2^2 N_3^2 + N_1^2 N_2^2 + N_1^2 \quad (6)$$

$$= N_1^2 N_2^2 N_3^2 \left(2\bar{S} + \frac{1}{N_3^2} + \frac{1}{N_3^2 N_2^2} \right)$$

From Eq. (6), it comes directly that one can minimise the memory usage by building the EKMR scheme such that:

$$N_1 < N_2 < N_3$$

Two approaches are investigated for the fragments cloud density propagation:

1. The sampled characteristics are propagated, and the density is estimated a posteriori for each required time snapshot.
2. The density is estimated from the initial samples and is directly propagated; the coordinates of the new set of ‘density samples’ correspond to the centre of the non-empty bins.

This second approach aims at exploiting the concentration of fragments in bounded regions of the phase space, to merge the information of the broad population of initial samples into a subset of ‘density samples’. This implies a more accurate snapshot of the initial density distribution, parity of the number of propagated characteristics. On the other hand, the coordinates of the samples belonging to the same bin are collapsed into a unique point in correspondence of the bin centre; this hypothesis constrains the domain partitioning, that must be sufficiently fine to avoid distorting impossibly the samples dynamics.

The two methods are applied to an example scenario representing the explosion of an upper stage in geostationary transfer orbit with the following parameters: $a = 24369$ km, $e = 0.72$, $i = 7$ deg, $\Omega = 328$ deg, $\omega = 243$ deg. All simulations consider 50 partitions in each hyper-direction composed of the five slow-varying orbital elements and A/m .

Figure 3 shows the density distribution at fragmentation epoch, while Figure 4 and Figure 5 show how the density distribution has changed 540 days after the fragmentation event, with the characteristics propagation and density propagation approaches, respectively. To assess the accuracy of the two methods, the cumulative distribution function is computed and compared with same distribution obtained from the population of samples, as shown in Figure 6. As expected, the first method accurately describes the fragments cloud density in all the phase space variables. The density propagation approach, instead, while capturing most of the density distribution, lacks accuracy in the argument of periapsis profile, which is the parameter most affected in the analysed orbital

region. It is worth noticing that the proposed simulation is a first trial; a more refined domain partitioning should

lead the density propagation method to approach the actual cumulative distribution.

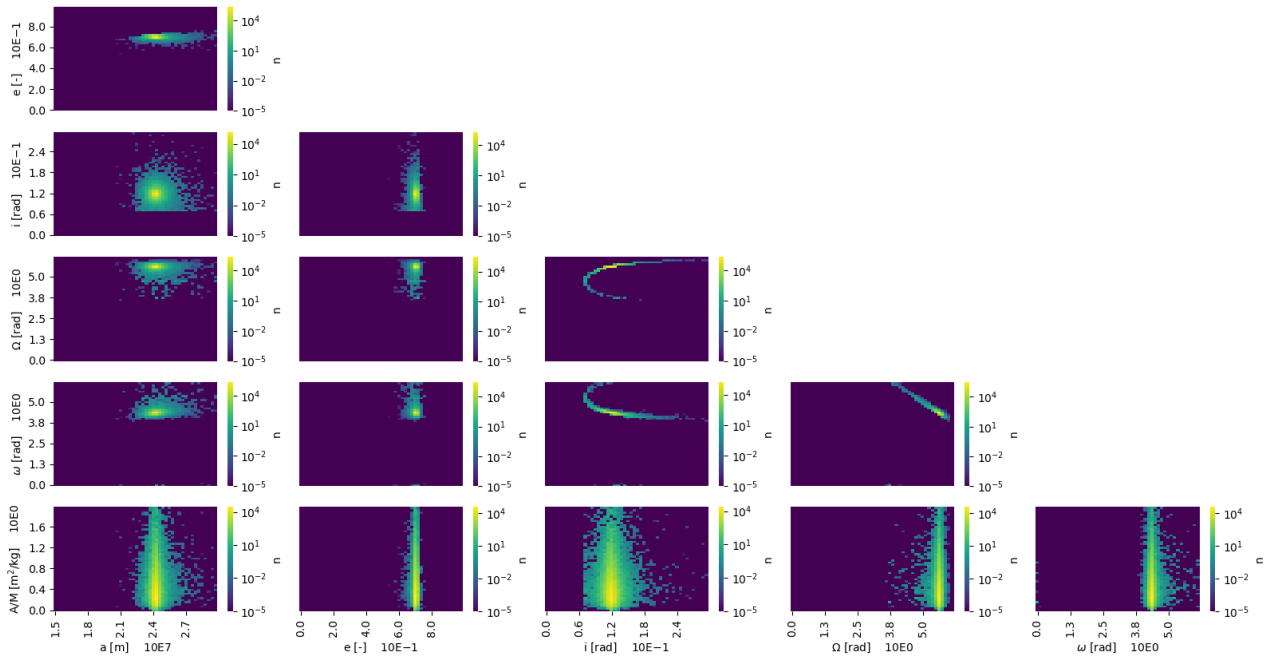


Figure 3: Density distribution at fragmentation epoch.

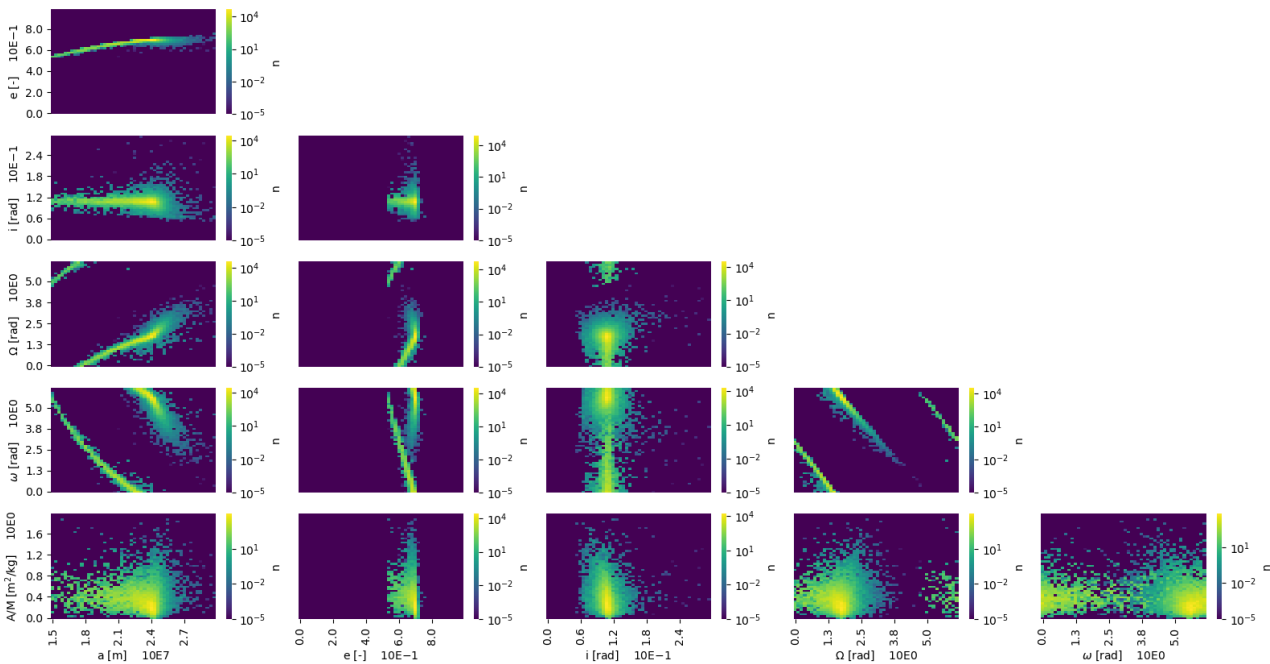


Figure 4: Density distribution 540 days after fragmentation obtained with characteristics propagation approach.

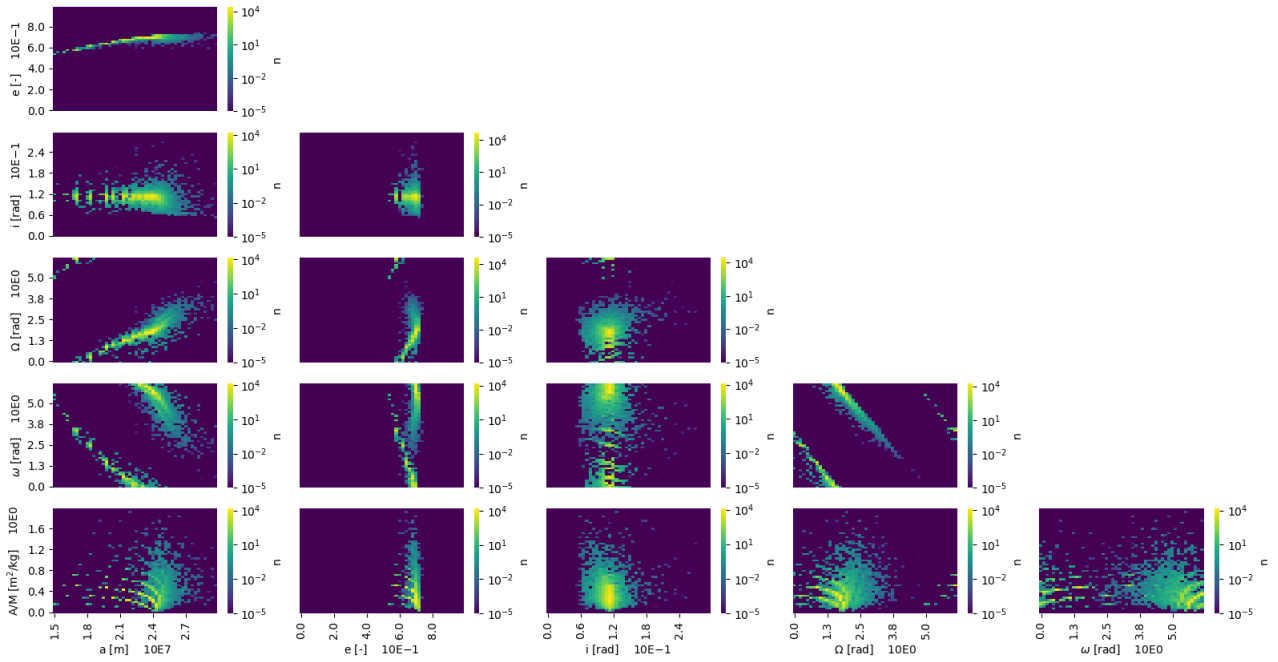


Figure 5: Density distribution 540 days after fragmentation obtained with density propagation approach.

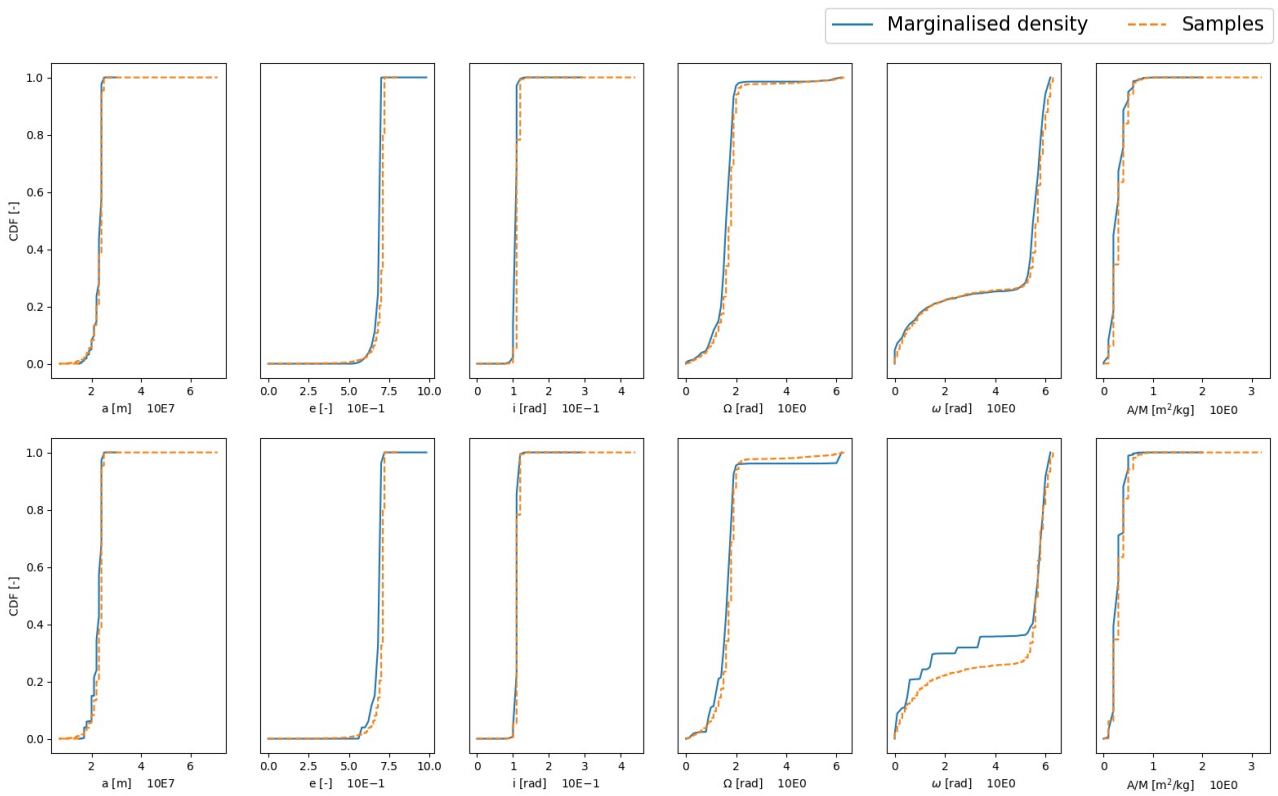


Figure 6: Cumulative distribution function 540 days after fragmentation for characteristics propagation (above) and density propagation (below) approaches.

2.3 Interface to propagator

The propagation of the dynamics for the continuum approach explained in Section 2.1 is performed through a semi-analytical trajectory propagator. The software tool will have a common interface to allow different propagators to be used. Current efforts are devoted in defining a propagator-agnostic interface that avoids lock-in with a specific propagator, and in adding support for additional propagators to enable testing and trade-offs. The main requirements for the propagator to be included are to allow for the efficient evaluation of the Jacobian, needed to solve Eq. (1), and to have the possibility to implement the density computation through the trace of the Jacobian matrix of the dynamics. Additionally, it is highly advisable from a performance point of view to have a thread-safe implementation, suitable for parallel propagation of the characteristics. Figure 7 shows the interface with the propagator. Currently, two options for propagators have been identified: the Planetary Orbital Dynamics (PlanODyn) semi-analytic orbit propagator, developed at Politecnico di Milano [7] and the Orekit space dynamics library, a free and open-source project lead by the CS Group [19].

The PlanODyn suite [7] is well suited for the cloud continuum propagation, as it was specifically extended to propagate many characteristics in parallel. PlanODyn models the Earth's gravitational field (up to 4th order and degree), atmospheric drag (derivative of Jacchia-77), Moon and Sun third-body perturbations and solar radiation pressure using the cannonball model. Despite its singular Keplerian formulation, it was shown that fragmentations from circular parent objects can be modelled too.

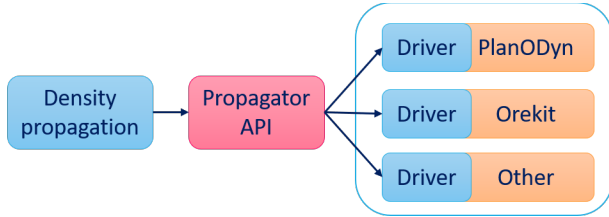


Figure 7: Interface with the propagator.

3 INDEX ESTIMATION AND INTERFACE REQUIREMENTS

The space debris index implemented in this tool will follow the definition of the ECOB index in Letizia et al. [12], which is defined as a risk indicator composed by a probability term (p) and an effect term (e), which considers the contribution of fragmentations on the sustainability of the space environment. The expression of the index is as follows:

$$I = p_c \cdot e_c + p_e \cdot e_e \quad (7)$$

where p_c and p_e represent the collision and explosion probabilities, and e_c and e_e represent the collision and explosion effects, respectively. Each term can be evaluated based on the characteristics of the object (i.e., mass and cross-section), its orbit and the mission scenario. The probability of collision (p_c) is evaluated using a flux-based model of the space debris environment and exploiting the analogy with the kinetic gas theory as follows:

$$p_c = 1 - e^{-\rho \cdot \Delta v \cdot A \cdot \Delta t} \quad (8)$$

where ρ is the debris density, Δv is the relative impact velocity, A is the cross-sectional area of the object and Δt is the time span considered. The value of the debris density and of the impact velocity are extracted from ESA MASTER, considering the debris population at a specified epoch. The cross-section of the object is obtained from a satellite database such as DISCOS.

When computing the collision probability, we only consider debris fluxes of particles whose diameter is large enough to generate a catastrophic collision. The criterion adopted is based on the energy of the collision, which should be greater than 40 J/g. In this way, we define a minimum required diameter that will generate a catastrophic collision. The relevant flux used in the computation of p_c is the cumulative flux associated to this diameter. However, the debris index calculation can also consider the possibility of performing Collision Avoidance Manoeuvres (CAM). With this respect, the general approach is to consider that objects larger than 10 cm can be tracked from Earth. Therefore, a satellite with collision avoidance manoeuvres capabilities will be able to avoid such debris. This is reflected in the collision term of the debris index by adding an upper limit on the particle diameter, which in turn result in a modified debris flux.

However, the traceability of debris particle also depends on the orbital altitude of the debris. In fact, the lower the altitude, the higher is the capability of telescopes of tracking smaller particles. The expression of the traceable diameter, d_t , as a function of the altitude is the following:

$$d_t = d_{ref} \cdot \left(\frac{h}{h_{ref}} \right)^2 \quad (9)$$

where h is the orbit altitude, $d_{ref} = 0.32$ m is a reference diameter, and $h_{ref} = 2000$ km a reference altitude. Using this expression in place of a constant diameter of 10 cm, the collision probability changes, particularly for lower altitudes. Figure 8 and Figure 9 show a comparison of collision probability maps in altitude and inclination for the same satellite but with different upper limits for the collision avoidance diameter. Figure 8 considers a

constant 10 cm threshold, while Figure 9 a variable one, based on Eq. (9). It is interesting to observe how in the second case, the lower altitude band, until about 900 km, shows a null collision probability. This is because at lower altitude smaller particle diameters can be tracked. This results in an upper diameter threshold that is smaller than the lower threshold needed to generate a catastrophic collision. Therefore, in this case, the satellite can avoid all the debris particles that can generate a catastrophic collision. This is of course valid assuming a 100% reliability of the CAM.

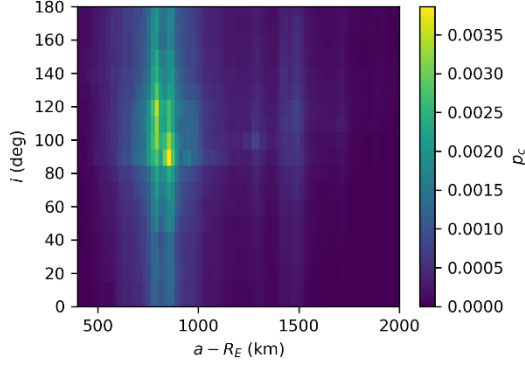


Figure 8: Collision probability map for a 1000 kg spacecraft with a 10 m² cross-section with constant 10 cm threshold.

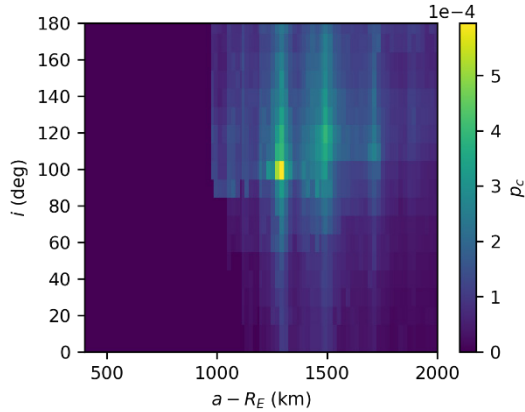


Figure 9: Collision probability map for a 1000 kg spacecraft with a 10 m² cross-section with a variable threshold.

The probability of explosion (p_e), instead, is derived from historical data gathered from the ESA DISCOS database in terms of epoch, altitude, event type, Id and class of the objects involved. Given the difference between the number of fragmentations occurred in payloads and rocket bodies, these two classes are considered separately in the modelling of p_e . In addition, fragmentation events due to collisions, deliberate destructions, atmospheric forces, and attitude are excluded. Figure 10 shows the data from DISCOS including only events involving rocket bodies and payload launched before 2020.

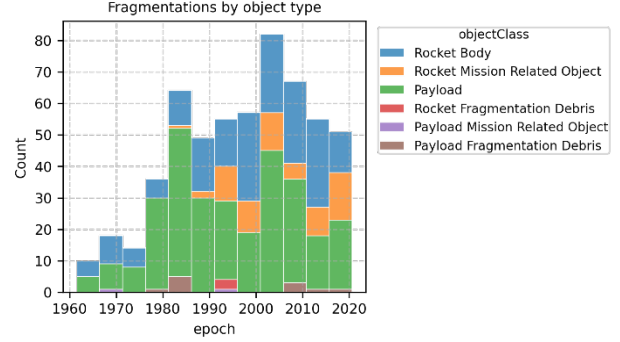


Figure 10. Fragmentation by object type from ESA DISCOS database.

Starting from the work in [14], the Kaplan-Meier estimator is used for estimating the explosion/survival probability for different classes of objects. This type of estimator allows considering a variable population that is, for our case, the removal of objects due to fragmentations and re-entries. The estimation will be updated on yearly basis (see Figure 11).

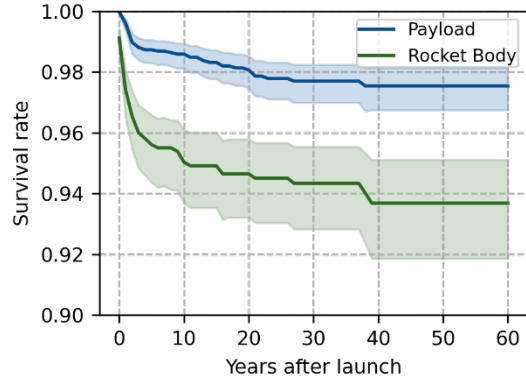


Figure 11. Example of survival rate for payload and rocket bodies.

The effect terms of both collisions (e_c) and explosions (e_e) depend on the characteristics of the fragmentation, and on the evolution of the cloud of debris and its interaction with the objects' population. Specifically, the resulting increase in the collision probability for operational satellites is used for the assessment of the consequences. The fragmentation is modelled following the NASA SBM [15], which provides the distribution of the generated fragments as a function of the object orbit and mass for both collisions and explosions. However, in this work the implementation proposed by Frey et al. is used that directly describes the distribution of the fragments in orbital elements exploiting the formulation in Gauss's planetary equations written for finite differences [16]. As proposed in the ECOB formulation [12] to assess the effects on the population of operational satellites, a set of representative targets is defined by considering the distribution of the cross-sectional area of the operational satellites on a semi-

major axis versus inclination grid.

The effect of fragmentations is evaluated by simulating a catastrophic collision for each grid cell and evaluating the increased collision probability for the target objects and the effect e_c then obtained with a weighted sum of the cumulative collision probability on each target, with the weights depending on the share of cross-sectional area represented by the representative object map cell. The MASTER ESA tool [17] is used to derive grid for the representative targets and effect maps (see Figure 12).

Figure 13 represents the weighted average position of the representative targets in inclination (C_i) and semi-major axis (C_a) weighted with their cross area. It is interesting to see how it changes in the years how it has been changing in the past few years due to the orbit injection of the SpaceX satellites.

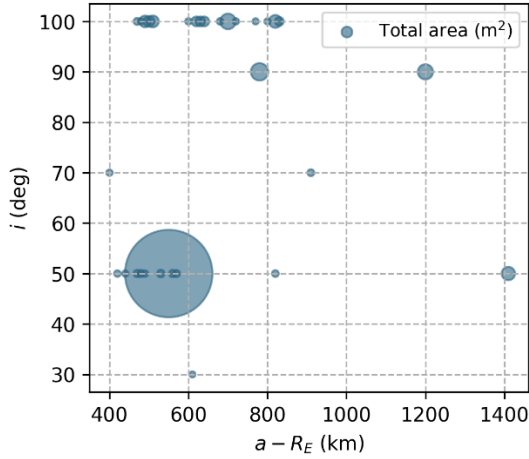


Figure 12. Representative objects in a semi-major axis and inclination grid. Data from ESA MASTER.

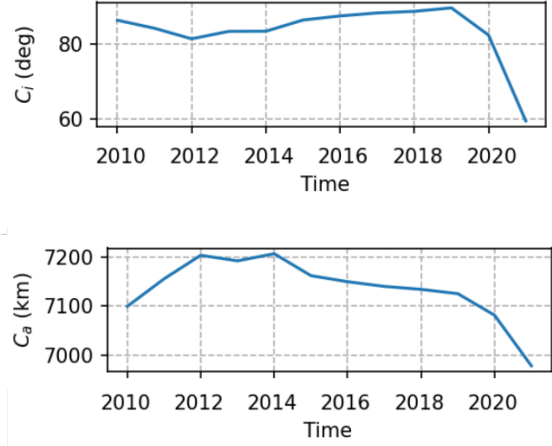


Figure 13. Weighted average position of the representative targets in inclination (C_i) and semi-major axis (C_a) weighted with their cross area. Data from ESA MASTER

The index in Eq. (7) is then assessed over time to get its cumulative value for the mission lifetime. As proposed in [13] the formulation include the reliability of post-mission disposal manoeuvres with a coefficient α .

$$I_t = \int_{t_0}^{t_{EOL}} I dt + \alpha \cdot \int_{t_{EOL}}^{t_e} I dt + (1 - \alpha) \cdot \int_{t_{EOL}}^{t_f} I dt \quad (10)$$

where t_{EOL} is the epoch at which the operational phase ends, t_e is the epoch at which the disposal ends and t_f is the epoch at which the object would naturally decay from its initial orbit.

Figure 14 represents the index estimation workflow that will be implemented within this project and highlights the interfaces with the available ESA tools. The inner computational core for the space debris index and the space capacity estimation will consist of the Staling-based cloud propagation module, the break-us modelling module, the single object mission profile module. These will be used within the debris index estimation module and the capacity evaluation module. As part of the project, the requirements for the interfaces with the ESA tools have been defined.

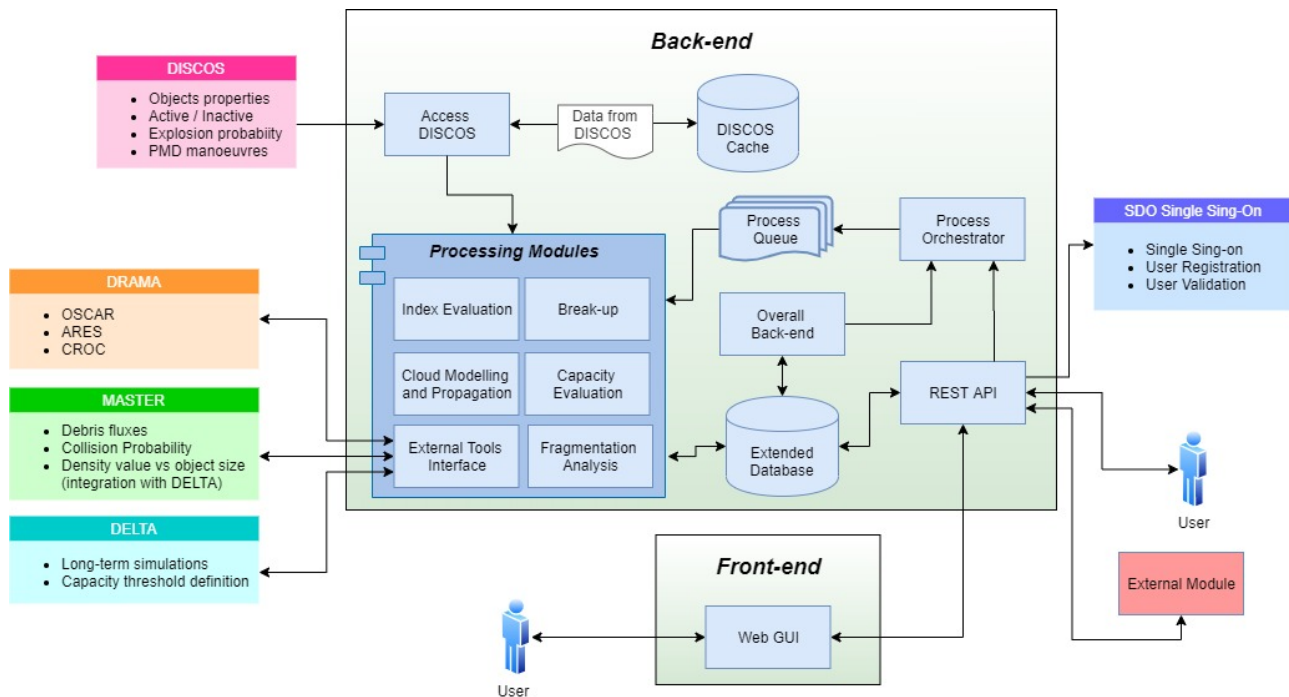


Figure 14. Index estimation workflow.

4 CONCLUSIONS

This paper presented the steps completed so far in the ESA-funded project for the design of a software to assess the impact of a space mission on the space environment. The Staling tool extension is being performed to be applied to computation of the space debris index. A space matrix approach has been implemented for efficient memory allocation during the propagation of a fragmentation cloud in 6 dimensions. The implementation of the space debris index based on the ECOB formulation is being performed with a particular attention on the definition of interfaces with existing ESA software and the orbit propagator.

As next steps some effort will be devoted to the development of the interfaces with ESA tools: DISCOS, MASTER, DRAMA. We will focus on the definition of the space capacity formulation and threshold. For this phase engagement with the space debris community will be very important.

5 REFERENCES

1. Maury T., Loubet P., Trisolini M., Gallice A., Sonnemann G., Colombo C., "Assessing the impact of space debris on orbital resource in Life Cycle Assessment: a proposed method and case study", *Science of the Total Environment*, 2019. <https://doi.org/10.1177/2053019614564785>
2. Colombo C., Letizia F., Trisolini M., Lewis H. G., Chanoine A., Duvernois P.-A., Austin J., Lemmens S., "Life cycle assessment indicator for space debris", 7th European Conference on Space Debris, Darmstadt, Germany, 18 - 21 Apr 2017.
3. Chun-Yuan Lin, Yeh-Ching Chung and Jen-Shiuh Liu, "Efficient data compression methods for multi-dimensional sparse array operations," First International Symposium on Cyber Worlds, 2002. Proceedings., Tokyo, Japan, 2002, pp. 62-69, doi: 10.1109/CW.2002.1180861.
4. Chun-Yuan Lin, Yeh-Ching Chung and Jen-Shiuh Liu, "Efficient Data Distribution Schemes for EKMR-Based Sparse Arrays on Distributed Memory Multicomputers," *The Journal of Supercomputing*, 34, 291-313, 2005.
5. Frey, S., "Evolution and hazard analysis of orbital fragmentation continua", PhD thesis, Politecnico di Milano, 2020, Supervisors: Colombo, C., Lemmens, S. and Krag., H.
6. Frey S., Colombo C., Lemmens S., "Application of density-based propagation to fragment clouds using the Starling suite", *1st International Orbital Debris Conference*, Houston, USA, 9 - 12 Dec 2019.
7. Colombo, C., "Planetary orbital dynamics (PlanODyn) suite for long term propagation in perturbed environment", 6th International

Conference on Astrodynamics Tools and Techniques (ICATT), Darmstadt, Germany, 14-17 March 2016

Flight Dynamics Applications," 4th ICATT, European Space Astronomy Center, Spain, 3-6 May 2010.

8. Krag, H., Lemmens, S., Letizia, F., "Space traffic management through the control of the space environment's capacity, " In Proceedings of the 1st IAA Conference on Space Situational Awareness (ICSSA), 2017.
9. Letizia, F., Colombo, C., and Lewis, H.G., "Analytical model for the propagation of small debris objects clouds after fragmentations," *Journal of Guidance, Control, and Dynamics*, Vol. 38, No. 8, pp. 1478-1491, 2015. doi: 10.2514/1.G000695
10. Letizia, F., Colombo, C., and Lewis, H.G., "Collision probability due to space debris clouds through a continuum approach," *Journal of Guidance, Control, and Dynamics*, Vol. 39, No. 10, pp. 2240-2249, 2016. doi: 10.2514/1.G001382
11. Letizia, F., Colombo, C., Lewis, H. G., Krag H., "Assessment of breakup severity on operational satellites," *Advances in Space Research*, Vol. 58, No. 7, pp. 1255-1274, 2016. doi: 10.1016/j.asr.2016.05.036
12. Letizia, F., Colombo, C., Lewis, H.G., Krag, H., "Extending the ECOB Space Debris Index with Fragmentation Risk Estimation," 7th European Conference on Space Debris, ESA/ESOC, Darmstadt, Germany, 18-21 Apr. 2017.
13. Letizia, F., Lemmens, S., Virgili, B. B., Krag, H., "Application of a debris index for global evaluation of mitigation strategies," *Acta Astronautica*, Vol. 161, pp. 348-362, 2019.
14. Letizia, F., Lemmens, S., Krag, H., "Environment capacity as an early mission design driver," *Acta Astronautica*, 2020, doi: 10.1016/j.actaastro.2020.04.041.
15. Johnson, N. L. and Krisko, P. H., "NASA's new breakup model of EVOLVE 4.0," *Advances in Space Research*, Vol. 28, Issue 9, pp. 1377-1384, 2001, doi: 10.1016/S0273-1177(01)00423-9.
16. Frey S., Colombo C., "Transformation of satellite breakup distribution for probabilistic orbital collision hazard analysis", *Journal of Guidance, Control, and Dynamics*, Vol. 44, No. 1, Jan. 2021. <https://doi.org/10.2514/1.G004939>
17. Flegel, S., Gelhaus, J., Möckel, M., Wiedemann, C., and Kempf, D., "Maintenance of the ESA MASTER Model", Final Report, 2011
18. Gelhaus, J., Kebschull, C., Braun, V., et al., "DRAMA - final report," Technical report, 2014.
19. Maisonobe, L., Pommier-Maurussane, V., "Orekit: An Open-source Library for Operational